1
2
3
4
5 **The roseoloviruses downregulate the protein tyrosine phosphatase PTPRC (CD45)**
6
7
8
9
10
11
12
13 *Melissa L. Whyte[1], Kelsey Smith[1], Amanda Buchberger[2,4], Linda Berg Luecke [4], Lidya*
14 *Handayani Tjan[3], Yasuko Mori[3], Rebekah L Gundry[2,4], and Amy W. Hudson[1#]*
15
16
17
18
19
20
21
22
23
24
25
26
27 *1: Department of Microbiology and Immunology, Medical College of Wisconsin, Milwaukee, WI*
28 *2. Department of Biochemistry, Medical College of Wisconsin, Milwaukee, WI*
29 *3. Division of Clinical Virology, Kobe University Graduate School of Medicine, Kobe, Japan*
30 *4: Current address: CardiOmics Program, Center for Heart and Vascular Research; Division of*
31 *Cardiovascular Medicine; and Department of Cellular and Integrative Physiology, University of*
32 *Nebraska Medical Center, Omaha, NE*
33
34
35
36 *[#]To whom correspondence should be addressed: ahudson@mcw.edu*
37
38
39
40 *Runnning title: Roseolovirus downregulation of CD45*
41
42
43
44
45
46

1

47   **Abstract**

48   Like all herpesviruses, the roseoloviruses (HHV6A, -6B, and -7) establish lifelong

49   infection within their host, requiring these viruses to evade host anti-viral responses.

50   One common host-evasion strategy is the downregulation of host-encoded, surface-

51   expressed glycoproteins. Roseoloviruses have been shown to evade host the host

52   immune response by downregulating NK-activating ligands, MHC class I, and the

53   TCR/CD3 complex. To more globally identify glycoproteins that are differentially

54   expressed on the surface of HHV6A-infected cells, we performed cell surface capture of

55   N-linked glycoproteins present on the surface of T cells infected with HHV6A, and

56   compared these to proteins present on the surface of uninfected T cells. We found that

57   the protein tyrosine phosphatase CD45 is downregulated in T cells infected with

58   HHV6A. We also demonstrated that CD45 is similarly downregulated in cells infected

59   with HHV-7. CD45 is essential for signaling through the T cell receptor and as such, is

60   necessary for developing a fully functional immune response. Interestingly, the closely

61   related β-herpesviruses human cytomegalovirus (HCMV) and murine cytomegalovirus

62   (MCMV) have also separately evolved unique mechanisms to target CD45. While

63   HCMV and MCMV target CD45 signaling and trafficking, HHV6A acts to downregulate

64   CD45 transcripts.

65   **Importance**

66   Human herpesviruses-6 and -7 infect essentially 100% of the world's population before

67   the age of 5 and then remain latent or persistent in their host throughout life. As such,

68   these viruses are among the most pervasive and stealthy of all viruses. Host immune

69   cells rely on the presence of surface-expressed proteins to identify and target virus-

70   infected cells. Here, we investigated the changes that occur to proteins expressed on

71   the cell surface of T cells after infection with human herpesvirus-6A. We discovered

72   that HHV-6A infection results in a reduction of CD45 on the surface of infected cells.

73   Targeting of CD45 may prevent activation of these virus-infected T cells, possibly

74   lengthening the life of the infected T cell so that it can harbor latent virus.

Introduction

Human Herpesvirus-6A (HHV6A) is a human-specific, T cell-tropic β-herpesvirus that is most closely related to the other members of the roseolovirus genus, HHV-6B and HHV-7, as well as human cytomegalovirus (HCMV). Primary infections with HHV-6 and -7 usually occur before the age of three and are often characterized by a high fever (1, 2). HHV-6 and -7 infect over 90% of the population, and like other herpesviruses, HHV-6 and -7 remain latent or establish lifelong infections in their hosts. As such, these viruses are among the most pervasive and stealthy of all viruses; they must necessarily excel at escaping immune detection throughout the life of the host, yet little is known about how these viruses so successfully escape host defenses.

The ability of host immune cells to detect virus-infected cells is largely dependent on interactions between proteins expressed on the surface of immune cells and those expressed on the surface of their targets. Viruses have necessarily evolved to alter the expression of these cell-surface-expressed proteins to evade detection by the host immune system. The herpesviruses, particularly the cytomegaloviruses, have long been known to employ devious strategies to interfere with expression of host-encoded surface-expressed proteins. For example, most herpesviruses, including HHV-6 and -7, interfere with antigen presentation by downregulating class I major histocompatibility complex (MHC) molecules from the surface of infected cells (4-13). Additionally, HCMV, the most closely-related virus to the roseoloviruses, encodes at least 5 different gene products and a miRNA that all participate in downregulation of natural killer (NK)-activating ligands, all in an effort to prevent natural killer cells from identifying and killing infected cells (14-18). We have found that HHV6A, -6B, and -7 each encode a single

4

98   gene product, U21, that acts as a multifunctional transmembrane glycoprotein to

99   downregulate not only multiple NK activating ligands, but also most class I MHC alleles

100   (12, 19-21).

101   Herpesviruses also target surface-expressed proteins to hinder the ability of immune

102   cells to perform their effector function. For example, herpesviruses inhibit T cell function

103   through the downregulation of co-stimulatory ligands like B7 and CD40, and

104   upregulation of co-inhibitory ligands such as PD-L1 and galectin-9 (22-32).

105   Herpesviruses also downregulate adhesion molecules, such as I-CAM, V-CAM, PECAM

106   and ALCAM, which can physically disrupt formation of the immune synapse and inhibit

107   T cell activation (33-37).

108   Since most herpesviruses are not T cell-tropic, changes in surface expression occur in

109   infected cells, and infected cells then exert their immunosuppressive effects through

110   interaction with uninfected T cells. But what happens to the surface of a T cell when it is

111   infected with a herpesvirus? The T cell-tropic roseoloviruses allow us to explore and

112   learn from alterations to the glycoprotein landscape on the surface of herpesvirus-

113   infected T cells. Herein, we applied a mass spectrometry strategy to identify and

114   quantify N-linked glycoproteins on the cell surface of HHV6A-infected T cells to yield the

115   first insights into how virus infection induces alterations in the cell surface landscape of

116   host cells. We discovered that the protein tyrosine phosphatase CD45 (PTPRC) is

117   downregulated from the surface of HHV6A-infected T cells. CD45 is expressed on the

118   surface of all nucleated cells of hematopoietic origin, where its activity is critical for the

119   proper function of immune cells (reviewed in (39-42)). The phosphatase activity of CD45

120   is required for successful signaling through the TCR (43-45), and as such, the

121   downregulation of CD45 could be an attractive strategy for viruses to impair T cell

122   signaling.

123   **Results**

124   *Cell-surface capture of CD45 in HHV6A-infected T cells*

125   To identify host-encoded surface-expressed proteins targeted by HHV6A, we performed

126   cell surface capture (CSC), a chemoproteomic approach for the specific identification of

127   cell surface *N*-glycoproteins (46-50). Using CSC and bioinformatic analysis tools, we

128   compared N-linked glycoproteins identified on the surface of T cells infected with

129   HHV6A to those identified on the surface of uninfected T cells (3, 38). To minimize

130   biological variability, we performed CSC in HHV6A-infected cell line. HHV6A infects

131   only a small number of cultured cell lines, and for these studies, we used JJhan cells, a

132   CD4+ T cell line variant of Jurkat cells (51).

133   We identified 605 cell surface N-linked glycoproteins on the surface of infected and

134   uninfected JJhan cells, including 594 human and 11 viral proteins. Strikingly, we

135   identified 47 unique peptides derived from the protein tyrosine phosphatase PTPRC

136   (CD45), spanning all 22 N-linked glycosylation sites (Fig. 1a). CD45-derived peptides

137   were consistently less abundant on the surface of HHV6A-infected JJhan cells across

138   multiple biological and technical replicates (Fig. 1b-d), suggesting that CD45 is

139   downregulated from the surface of HHV6A-infected JJhan cells.

140   *Localization and steady-state expression of CD45 in HHV6A-infected T cells*

6

141 To independently validate the

142 downregulation of CD45

143 observed in our mass

144 spectrometry experiments, we

145 examined surface-expression of

146 CD45 in HHV6A-infected cells by

147 flow cytometry. We infected

148 JJhan cells with a recombinant,

149 bacterial artificial chromosome

150 (BAC)-derived HHV6A virus

151 encoding soluble green

152 fluorescent protein (GFP), which

153 allowed us to identify actively-

154 infected cells (52). In uninfected

155 JJhan cells, we observed a single

156 population of CD45-expressing

157 cells, while in HHV6A-infected

158 JJhan cells, we observed

Figure 1. Mass spectrometry data for CD45. (a) Graphical representation of CD45 protein with extracellular N-linked glycopeptides identified by CSC indicated. This approach specifically enriches and identifies N-glycopeptides from the extracellular domain of cell surface proteins. Image generated using Protter (3). (b-d) Label-free quantitation data for CD45. Representative peaks of a peptide (YAnITVDYLYNK, where n is the site of *N*-glycosylation) detected across individual replicate analyses (b) and three replicate analyses (including technical replicates) (c) for each sample group, showing CD45 is more abundant in control compared to infected cells. Each color (blue, purple, and red) are associated with the peak area from the [M]+0, [M]+1, and [M]+2 isotopic peaks, respectively. [M] is the monoisotopic mass. (d) Summary of peak areas for all 67 peptide observations for CD45 across all technical and biological replicates. Each line is a different peptide. BR: biological replicate; TR: technical replicate. Results shown in b-d were generated using Skyline (38).

159 reduced surface expression of CD45 (Fig. 2a), consistent with our mass spectrometry

160 finding that the presence of CD45 is diminished on the surface of HHV6A-infected cells.

161 CD45 is expressed as multiple different isoforms in human cells (53-55). To determine

162 whether all isoforms of CD45 are downregulated in HHV6A-infected JJhan cells, we

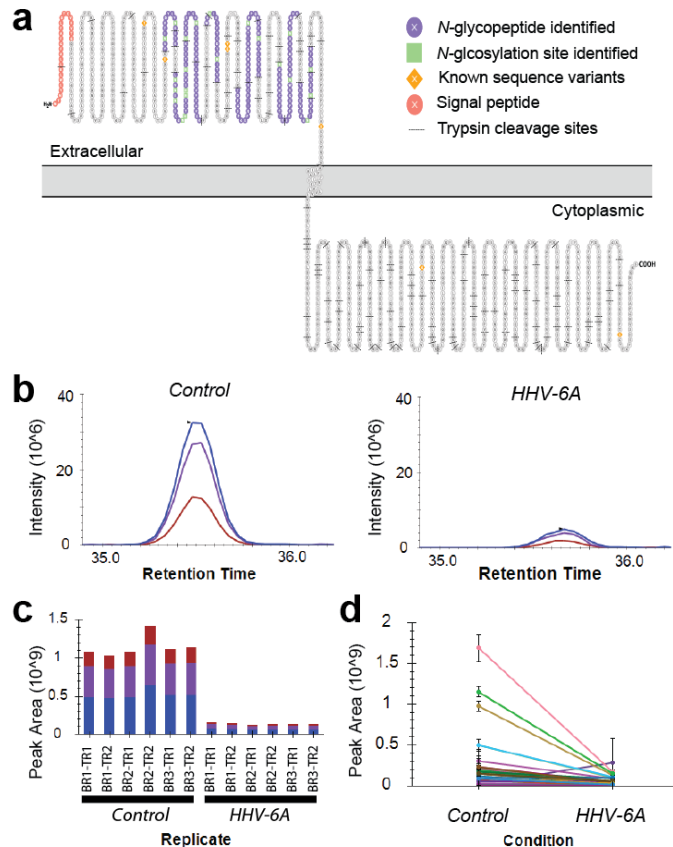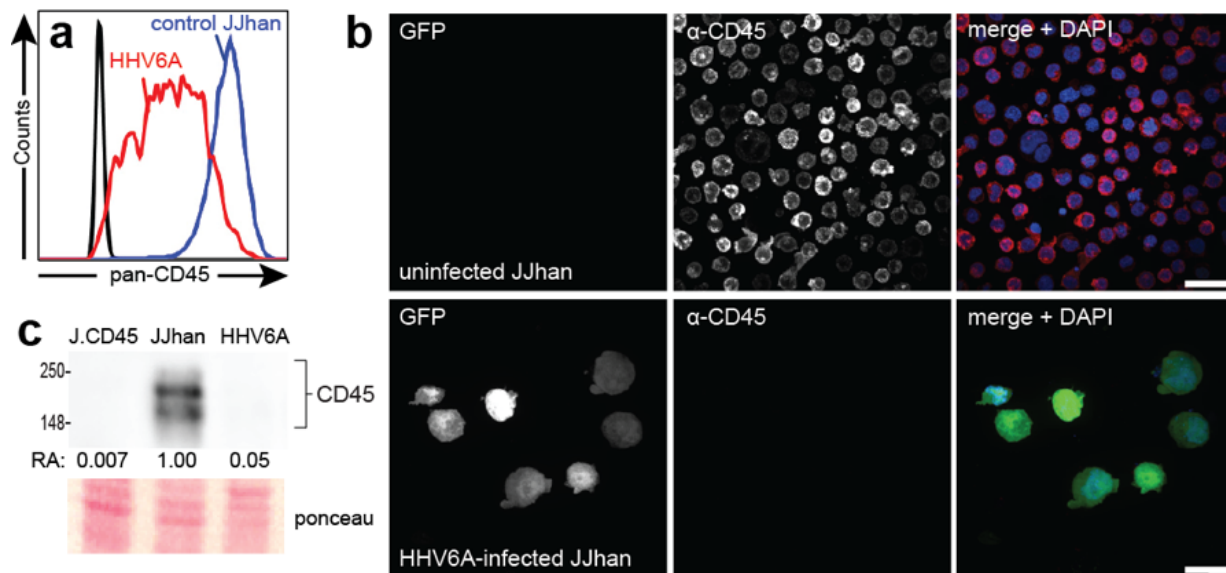163 labeled cells with antibodies directed against the CD45 isoforms commonly expressed

7

Figure 2. CD45 is downregulated in HHV6A-infected cells. (a) Flow cytometric analysis of HHV6A-infected JJhan cells (red) and uninfected JJhan cells (blue). HHV6A-infected cells were gated on as GFP+. Live cells were labeled with an antibody directed against CD45. (b) Confocal immunofluorescence microscopy images showing uninfected JJhan cells (top panels) and HHV6A-infected (GFP+) JJhan cells (bottom panels) that were fixed, permeabilized, and labeled with an antibody directed against CD45. Images were taken at 100X magnification and are shown as maximum intensity projections. Scale bar = 20 μm. (c) Immunoblot analysis of CD45 in whole cell lysates generated from J.CD45 cells (negative control), uninfected JJhan cells, and HHV6A-infected JJhan cells. Protein was normalized to total protein for each lane. RA : relative abundance. Abundance is calculated relative to uninfected JJhan cells. Ponceau shows total protein loaded per lane.

164   in Jurkat cells, the parental cell line of JJhan cells (56). CD45-RO, -RB, and -RC were

165   all downregulated in HHV6A-infected JJhan cells relative to uninfected JJhan cells (Fig.

166   S1), suggesting the downregulation of CD45 from the surface HHV6A-infected JJhan

167   cells is not specific to any one CD45 isoform.

168   Viruses often reroute the intracellular trafficking of surface-expressed proteins from the

169   cell surface to alter host cell biology. For example, the HHV6A U24 gene product

170   downregulates the T-cell receptor (TCR)/CD3 by stimulating endocytosis of the receptor

171   resulting in relocalization of TCR/CD3 from the cell surface to endosomes, and U21

172   reroutes class I MHC molecules to lysosomes (13, 57). We therefore sought to

173   determine whether the reduction in surface-expressed CD45 observed in HHV6A-

174   infected cells was the result of a redistribution of CD45 within the cell. To examine the

175   localization of CD45, we performed immunofluorescence microscopy of permeabilized

8

176   cells labeled with an antibody directed against human CD45. As expected, CD45 was

177   localized to the plasma membrane in uninfected JJhan T cells. In HHV6A-infected

178   JJhan cells, however, we observed a striking disappearance of CD45 labeling (Fig. 2b).

179   To better quantify the downreguation of CD45 in HHV6A-infected JJhan cells, we next

180   examined steady-state levels of CD45 protein by immunoblot analysis of whole-cell

181   lysates generated from uninfected or HHV6A-infected JJhan cells. Consistent with our

182   immunofluorescence microscopy data (Fig. 2b), immunoblot analysis showed a 95%

183   reduction in CD45 protein in HHV6A-infected JJhan cells relative to uninfected JJhan

184   cells (Fig. 2c). Taken together, these results demonstrate that CD45 is not only

185   downregulated from the surface of HHV6A-infected JJhan cells but is also depleted

186   from HHV6A-infected cells.

187   *CD45 expression in HHV7-infected T cells*

188   The HHV6A genome is almost entirely co-linear with the two other roseolovirus

189   genomes HHV-6B and HHV-7 (58, 59). As such, we reasoned that HHV-6B and HHV-7

190   infection may also result in CD45 downregulation. To determine whether CD45 is

191   downregulated in HHV7-infected cells, we evaluated the localization of CD45 in HHV7-

192   infected SupT1 cells by immunofluorescence microscopy. Since a recombinant GFP-

193   containing BAC containing the coding sequence of HHV-7 is not yet available, we

194   identified HHV7-infected cells using an antibody directed against the U21 gene product

195   from HHV-7 (Fig. 3, green). Similar to cells infected with HHV6A (Fig. 2b), HHV7-

196   infected SupT1 cells showed reduced CD45 labeling (Fig. 3, bottom panels as

9

197 compared to

198 uninfected

199 SupT1 cells

200 (Fig. 3, top

201 panels),

202 suggesting that

203 the ability to

204 downregulate

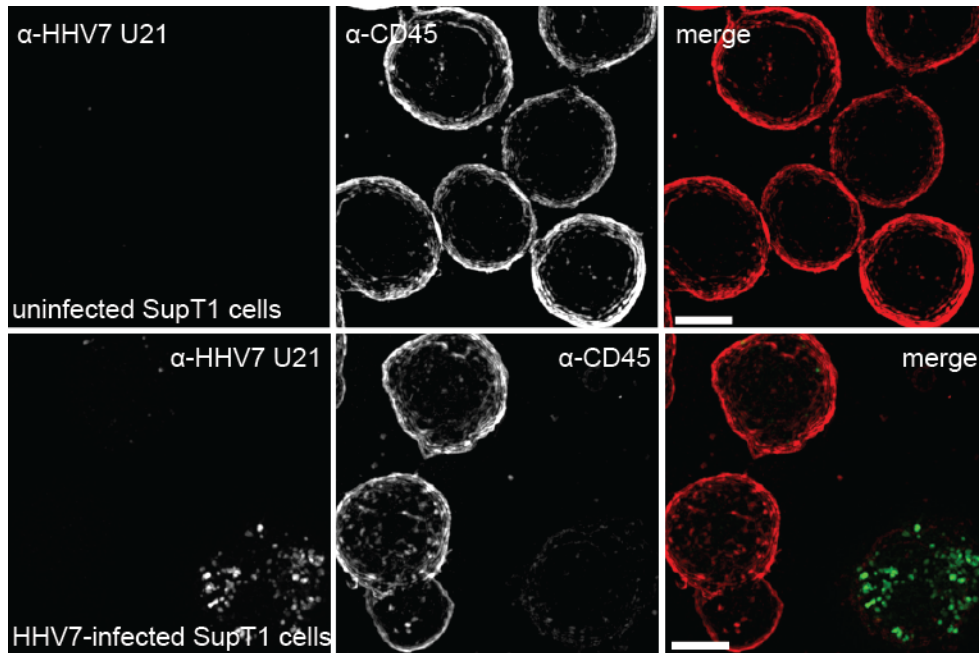205 CD45 is

206 common to all

207 roseoloviruses.

Figure 3. CD45 is downregulated in HHV7-infected T cells. Structured Illumination 3-dimensional microscopy images showing uninfected control T cells (top panels) and HHV7-infected T cell (bottom panels). Fixed and permeabilized cells were labeled with an antibody directed against the U21 open reading frame (ORF) from HHV7 (green) and an antibody directed against human CD45 (red). Images were taken at 100X and are shown as maximum intensity projections. Scale bar = 5 μm.

208 *CD45 protein stability in HHV6A-infected T cells*

209 Viruses often employ the strategy of degrading host proteins involved in the host

210 response to virus infection. For example, the murine cytomegalovirus m42 gene product

211 induces internalization and subsequent proteasomal degradation of CD45 (60). To

212 further investigate the mechanism by which CD45 is downregulated in HHV6A-infected

213 JJhan cells, we examined the stability of CD45 in the presence of proteasomal and

214 lysosomal protease inhibitors.

215 Lysosomal protease function is compromised at a more neutral pH, thus stabilization of

216 a protein in the presence of the weak base ammonium chloride (NH_4Cl) would suggest

217 the involvement of lysosomal proteases in its turnover. Likewise, stabilization of a

218 protein in the presence of the peptide-aldehyde MG-132, which selectively inhibits

10

219   proteolytic activity of the 26S

220   proteasome, would suggest

221   involvement of proteasomal

222   proteases in the turnover of that

223   protein. We separately inhibited

224   lysosomal and proteasomal

225   protein degradation, treating

226   cells with NH₄Cl or MG-132, and

227   assessed steady-state CD45

228   protein levels by immunoblot

229   analysis. In cells treated with a

230   DMSO vehicle control, we

231   observed a 95% reduction in

232   CD45 abundance in HHV6A-

233   infected cells (Fig 4a), which is

Figure 4. CD45 is downregulated at the RNA level in HHV6A-infected T cells.
(a) Immunoblot analysis showing steady-state abundance of CD45 protein in uninfected JJhan cells, or HHV6A-infected cells under different conditions (DMSO vehicle control, MG-132, or NH4Cl treatment for 19 hours). Equal protein was loaded in each lane, and CD45 abundance was calculated relative to uninfected JJhan cells for each treatment. RA = relative abundance. Ponceau-stained lanes visually illustrate equal protein loading. (b) CD45 RNA abundance in 293T cells (negative control), uninfected JJhan cells, or HHV6A-infected cells. CD45 RNA abundance is calculated relative to a cellular control gene and shown here relative to uninfected JJhan cells. Data shown is from a single representative biological replicate, performed in technical triplicate for each sample, mean +/- SD. **** = p < 0.0001.

234   similar to what we observed in untreated cells (Fig. 2c), suggesting the dimethyl

235   sulfoxide (DMSO) vehicle does not affect degradation of CD45. We observed a similar

236   reduction in CD45 in cells treated with MG-132 or NH₄Cl (Fig. 4a).

237   We also examined localization of CD45 in HHV6A-infected cells treated with MG-132 or

238   NH₄Cl by immunofluorescence microscopy. As expected, we observed surface-

239   localization of CD45 in untreated, uninfected JJhan cells (Fig. S2, panel a). We also

240   observed surface-localization of CD45 in uninfected JJhan cells treated with a DMSO

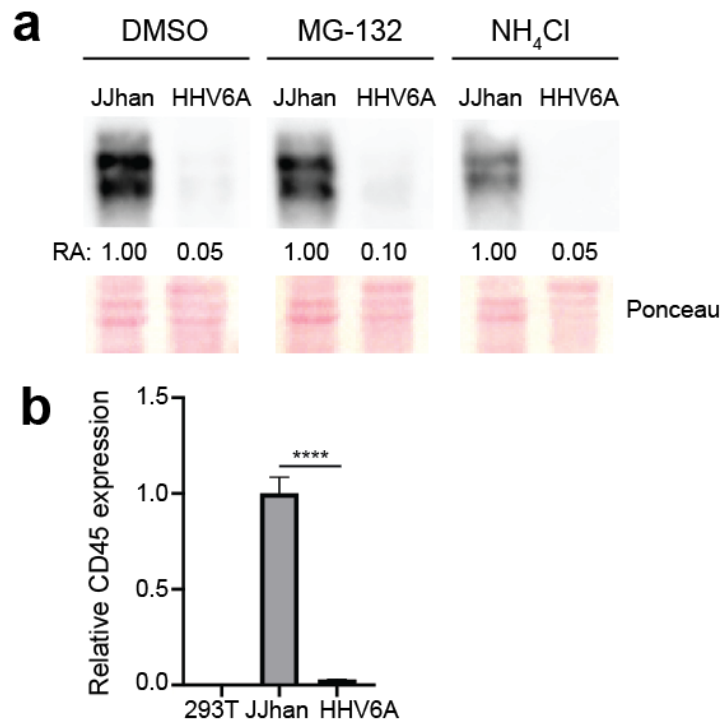241   vehicle, MG-132, or NH₄Cl (Fig. S2, panels b, c, and d, respectively), suggesting CD45

11

242   localization is not affected by treatment with MG-132 or NH4Cl outside the context of an

243   HHV6A infection. Consistent with the immunoblot data, there was little to no CD45

244   labeling present in untreated HHV6A-infected JJhan cells (Fig. S2, panel e). Similarly,

245   there was little to no CD45 labeling in HHV6A-infected treated with a DMSO vehicle,

246   MG-132, or NH4Cl (Fig. S2, panels f, g, & h, respectively). Taken together, these results

247   suggest that the downregulation of CD45 in HHV6A-infected JJhan cells occurs by

248   some method other than protein degradation.

249   *CD45 gene expression in HHV6A-infected T cells*

250   Because CD45 was not stabilized in the presence of proteasomal or lysosomal

251   inhibitors, we hypothesized that CD45 was downregulated at the transcript level in

252   HHV6A-infected T cells. To test this hypothesis, we quantified CD45 mRNA in

253   uninfected and HHV6A-infected JJhan cells by quantitative reverse transcriptase-

254   polymerase chain reaction (qRT-PCR). CD45 mRNA levels were greatly reduced in

255   JJhan cells infected with HHV6A as compared to uninfected JJhan cells (Fig. 4b),

256   suggesting that CD45 transcripts are downregulated in HHV6A-infected JJhan cells.

257   **Discussion**

258   Herpesviruses, as life-long pathogens, are especially masterful at reprogramming host

259   cells to create a more hospitable environment. Perhaps the greatest challenge to a virus

260   is the detection and killing of its host cell by immune cells. As discussed, the

261   herpesviruses encode multiple gene products that alter host cell biology to prevent the

262   identification of infected cells. These measures are not entirely sufficient, however, and

263   viruses also strategize to target immune cells to inhibit their functional capacity. One

12

264   way viruses can inhibit these processes is by targeting the proteins that are important

265   for immune cell function, such as the protein tyrosine phosphatase CD45.

266   CD45 is expressed on the surface of all nucleated cells of hematopoietic origin, where

267   its activity is critical for the proper function of immune cells (reviewed in (39-42)). In T

268   cells, CD45's primary substrates are Src family kinases (61-63). CD45

269   dephosphorylates the inhibitory phosphotyrosine residue on the Src kinase Lck, leaving

270   the kinase in a 'primed' state, so that it can be activated through T cell receptor (TCR)

271   signaling (62). The phosphatase activity of CD45 is required for successful signaling

272   through the TCR (43-45), and as such, the downregulation of CD45 could be an

273   attractive strategy for viruses to inhibit T cell signaling.

274   Here we describe the downregulation of CD45 by two roseoloviruses, HHV6A and HHV-

275   7. Expression of CD45 is markedly reduced in HHV6A-infected JJhan cells and HHV7-

276   infected SupT1 cells. While we do not yet fully understand the functional consequences

277   of CD45 downregulation in roseolovirus-infected cells, we can gather clues from three

278   other viruses also known to target CD45: human cytomegalovirus (HCMV), human

279   adenovirus, and murine cytomegalovirus (MCMV).

280   CD45 is targeted by HCMV pUL11 (64). The extracellular domain of pUL11, which is

281   expressed on the surface of HCMV-infected epithelial cells or fibroblasts, interacts with

282   CD45 on nearby uninfected T cells. The interaction between pUL11 and CD45 inhibits

283   the phosphatase activity of CD45, which in turn impairs TCR signaling and ultimately, T

284   cell proliferation (64, 65). Inhibition of CD45 by pUL11 also results in an increase in

285   production of the anti-inflammatory cytokine IL-10 (65). In HHV6A infection, the

13

286   concentration of secreted IL-10 protein was shown to be increased during HHV6A

287   infection at timepoints up to 72 hours post-infection (66, 67). Since the inhibition of

288   CD45 during HCMV infection results in an increase in IL-10 production (65), it is

289   tempting to speculate that the downregulation of CD45 we observe in HHV6A-infected T

290   cells may be involved in the increase in IL-10 levels shown to occur during HHV6A

291   infection.

292   Another virus that devotes an open reading frame to the downregulation of CD45 is

293   Adenovirus19a (Ad19a). Ad19a E3/49K protein is cleaved to a secreted form (sec49K)

294   that interacts with CD45 on nearby uninfected NK cells and T cells. Sec49K-mediated

295   inhibition of CD45 suppresses T cell activation and signaling, resulting in diminished

296   production of the anti-viral cytokine IFN-γ, and inhibition of NK cell activation (68). After

297   HHV6A infection of stimulated peripheral blood mononuclear cells, the production of

298   IFN-γ was also reported to be reduced (66). Since inhibition of CD45 function during

299   adenovirus infection results in a decrease in IFN-γ production (68), it is possible that the

300   decrease reported in IFN-γ production during HHV6A infection may occur as a result of

301   CD45 downregulation in infected T cells.

302   Unlike HCMV pUL11 and Ad19a sec49K, which act extracellularly to inhibit CD45,

303   MCMV encodes a protein, m42, that induces the internalization and degradation of

304   CD45 within MCMV-infected macrophages (60). MCMV m42 acts as an adaptor or

305   activator of HECT3 E3 ubiquitin ligases, and through ubiquitination, m42 marks CD45

306   for lysosomal degradation (60). The functional outcome of m42-mediated

307   downregulation of CD45 in MCMV-infected macrophages is unclear. HHV6A-mediated

308   downregulation of CD45 is similar to MCMV-mediated downregulation of CD45, in that

309   these viruses downregulate CD45 from within infected cells, as opposed to acting on

310   CD45 *in trans* on the surface of nearby uninfected cells. As yet, the functional outcome

311   of downregulating CD45 within either of these infected immune cells remains elusive.

312   The roseolovirus genomes lack positional or functional homologs of MCMV m42 or

313   HCMV pUL11, and unlike HCMV, MCMV, and Ad19a, HHV6A infection results in the

314   dramatic transcriptional downregulation of CD45. HHV6A therefore downregulates

315   CD45 by a novel mechanism. The separate evolution of four unique mechanisms to

316   target a single host protein strongly suggests that CD45 is an important viral target,

317   though its impact is unclear: how might the roseoloviruses benefit from the

318   downregulation of CD45 in infected T cells? As discussed above, while the influence of

319   CD45 downregulation on cytokine production would certainly benefit HHV6A, it is

320   important to note that HHV6A preferentially infects T cells. Since it takes days to mount

321   a virus-specific T cell response, during a primary infection, the T cells that HHV6A

322   infects are not likely to be HHV6A-specific. Therefore, downregulation of CD45 in

323   infected T cells would not directly impair activation of T cells responding to HHV6A

324   infection. Instead, downregulation of CD45 may be a means to inhibit activation of the

325   HHV6A-infected T cell, possibly preventing activation-induced cell death, and creating a

326   host cell environment conducive to harboring latent virus. Future work is focused on

327   identification of the HHV6A gene products involved in the transcriptional regulation of

328   CD45 and exploring the functional consequences of CD45 downregulation in

329   roseolovirus-infected T cells.

330

331 **Materials & Methods**

332 *Cell lines and viruses*

333 JJhan, ND10^{depl} JJhan, and J.CD45 T cells were cultured in RPMI-1640 medium

334 (ThermoFisher Scientific, Waltham, MA) supplemented with 5% fetal bovine serum

335 (FBS) and 2 mM L-glutamine. JJhan cells depleted of ND10 (ND10^{depl} JJhan cells) were

336 the kind gift of Dr. Benedikt Kaufer (Freie Universität, Berlin, Germany) (69). J.CD45

337 cells (CD45 -negative Jurkat cells) were kindly provided by Dr. Arthur Weiss (UCSF,

338 San Francisco, CA) (70). 293T cells were cultured in Dulbecco's modified Eagle

339 medium (DMEM) (Invitrogen, Carlsbad, CA) supplemented with 5% FBS, 5% newborn

340 calf serum, and 2 mM L-glutamine. The HHV6A virus used in these studies is a

341 recombinant HHV6A virus (strain U1102) generated from a bacterial artificial

342 chromosome (BAC) containing the HHV6A genome with GFP inserted between the U53

343 and U54 ORFs (71). Infectious HHV6A virus was generated by electroporating HHV6A-

344 GFP BAC DNA into JJhan T cells. HHV6A virus was propagated by mixing uninfected

345 ND10-depleted Jhan cells with infected JJhan cells once HHV6A-infected JJhan cells

346 were >80% GFP+. HHV6A-infected and uninfected JJhan cells as well as J.CD45 cells

347 were stimulated with 3.75 ug/ml Phytohemagglutinin (PHA-P) and 9 ug/ml

348 hydrocortisone. HHV6A-infected cells used for experiments in this study were ≥70%

349 GFP+ at the time of harvest. SupT1 cells were cultured in RPMI-1640 medium

350 supplemented with 2.5% FBS and 2 mM L-Glutamine. HHV-7 infection (strain SB) was

351 performed by co-culture of HHV7-infected SupT1 cells with uninfected SupT1 cells.

352

16

353   *Antibodies & reagents*

354   The monoclonal anti-human CD45 antibody (clone S5-Z6, Santa Cruz Biotechnology,

355   Dallas, TX) was used for flow cytometry (1 ug/ 1 x10^6 cells), immunofluorescence

356   microscopy (1:50), and immunoblotting (1:50). The monoclonal anti-CD45 antibody

357   (clone MEM-28, Millipore-Sigma, St. Louis, MO) was used for immunofluorescence

358   microscopy (1:200). The polyclonal antibody MCW62 (U21-N) was raised against the N-

359   terminus of HHV-7 U21 (1:400) (72). AlexaFluor-405, -488, -594, and -647-conjugated

360   goat-anti mouse and rabbit secondary antibodies were used at dilutions recommended

361   by the manufacturer (ThermoFisher Scientific). Chemicals were purchased from Sigma

362   Millipore unless otherwise noted.

363   *Identification of cell surface N-glycoproteins*

364   Cell Surface Capture (CSC) was applied to control JJhan and HHV6A-infected JJhan T

365   cells (10 million cells per replicate, three biological replicates per condition). Briefly,

366   extracellular glycans on intact cells were oxidized using sodium meta-periodate, and the

367   resulting aldehydes were labelled with biocytin hydrazide to form a 'handle' for

368   enrichment. Cells were then lysed, proteins enzymatically digested, and biotinylated

369   glycopeptides were enriched using streptavidin beads. *N*-glycopeptides were then

370   selectively released by Peptide-N-Glycosidase F (PNGase:F) and analysed by mass

371   spectrometry. Here, CSC was performed as previously described in detail (47-50), with

372   the exception that glycopeptide enrichment and bead washing was performed using an

373   epMotion 5073m (Eppendorf, Hamburg, Germany). For each sample, 750 μg of total

374   peptide was diluted in binding buffer (80 mM sodium phosphate, 2 M NaCl, 0.2% Tween

375   20, pH 7.8) and incubated with 100μL of GenScript Streptavidin MagBeads (GenScript,

376   Piscataway, NJ) for 1 h with mixing. Beads were then washed sequentially with: (1) 2%

377   sodium dodecyl sulfate in ultrapure water, (2) 80 mM sodium phosphate, 2 M NaCl,

378   0.2% Tween 20, pH 7.8, (3) 100 mM sodium carbonate, (4) 80% isopropyl alcohol in

379   ultrapure water, (5) ultrapure water, and (6) 50 mM ammonium bicarbonate. Peptides

380   were released by digestion with PNGase F (Promega, Madison, WI) overnight at 37 °C

381   with vortexing. Deglycosylated peptides were cleaned and desalted using the SP2

382   procedure (73). Peptide Retention Time Calibration (PRTC) Mixture (ThermoFisher

383   Scientific) was added to each sample at a final concentration of 2 nM to enable

384   retention time calibration and assessment of instrument performance throughout the

385   acquisition. A "pooled QC" mixture was generated by combining equal portions of each

386   sample. Individual samples were queued in a randomized order within a technical

387   injection series with two technical replicates each. Pooled QC samples were analyzed

388   at the beginning and end of each technical injection series. Samples were analyzed by

389   liquid chromatography tandem mass spectrometry (LC-MS/MS) using a Dionex UltiMate

390   3000 RSLCnano system in-line with an Orbitrap Fusion Lumos (ThermoFisher

391   Scientific), and data were analysed with Proteome Discoverer 2.3 and Skyline (38).

392   Normalized quantitation ratios were determined by comparisons of each sample type to

393   the pooled QC.

394   *Immunofluorescence microscopy*

395   T cells were adhered onto poly-L-lysine-coated glass coverslips as described in (74)

396   and permeabilized in 0.5% saponin in PBS + 3% BSA + 880 uM Ca^{2+} + 490 uM Mg^{2+}.

397   Permeabilized cells were incubated with primary antibodies, washed, and then

398   incubated with secondary antibodies conjugated to a fluorophore. 4′,6-diamidino-2-

399   phenylindole (DAPI) was added to the final PBS wash at 1 ug/ml to stain DNA.

400   Superresolution microscopy was performed on a Nikon Structured-Illumination

401   Microscope (N-SIM; Nikon) and NIS-Elements AR imaging and 3D reconstruction

402   software (v. 5.11) (Nikon Instruments Inc, Melville, NY). Images were taken using a

403   Nikon 100X Oil-immersion lens (CFI Apo SR TIRF 1.49 NA) and an Andor iXon+897

404   EMCCD camera. Confocal microscopy was performed on a Nikon Eclipse Ti2

405   microscope equipped with a W1 Spinning Disc, Orca Flash CMOS camera, and 100X

406   oil-immersion objective (CFI Plan Apo λ 1.49 NA), and NIS-Elements AR imaging and

407   3D reconstruction software (v. 6.0).

408   *Flow cytometry*

409   Cells were incubated with primary antibodies in 1% bovine serum albumin (BSA) in

410   DMEM -phenol red for 30 min on ice, washed, and incubated with secondary antibodies.

411   Flow cytometry was performed using an LSRII flow cytometer (BD Biosciences, San

412   Jose, CA). Data was analyzed using FlowJo analysis software (v. 10.7, BD

413   Biosciences). Infected cells were selectively analyzed by GFP+ gating. Non-viable cells

414   were excluded from all flow cytometric analyses.

415   *Immunoblotting*

416   Cell lysates were prepared using 1% Triton Tx-100 lysis buffer supplemented with 62.5

417   U/ml Benzonase and 174 μg/ml phenylmethylsulfonyl fluoride (PMSF) followed by the

418   addition of an equal volume of 2% sodium dodecyl sulfate (SDS) and 100 mM Tris-HCl

419   (pH 7.4). Lysates were normalized to total protein concentration as determined by

19

420   bicinchronic acid (BCA) assay (Pierce, Rockford, IL). Lysates were resolved by SDS-

421   PAGE and transferred to BA-85 nitrocellulose membrane (Cytivia, Marlborough, MA).

422   Membranes were incubated with primary antibodies, followed by HRP-conjugated

423   secondary antibody (BioRad Laboratories, Hercules, CA). Bands were visualized using

424   SuperSignal West Pico reagent (ThermoFisher Scientific) imaged with an Azure c600

425   gel documentation system and quantified using AzureSpot software (v2.2.167) (Azure

426   Biosystems, Dublin, CA).

427   *Inhibition of protein degradation*

428   HHV6A-infected or uninfected JJhan cells were incubated in RPMI in 50 mM NH_4Cl, 100

429   nM MG-132, or a DMSO control for 19 hours. Cells were then divided for use in

430   immunofluorescence microscopy or immunoblot analysis.

431   *qRT-PCR*

432   Cells were lysed in TRIzol (Invitrogen, Carlsbad, CA) according to the manufacturer's

433   instructions. Approximately 2 ug of RNA was treated with an AccuRT Genomic DNA

434   Removal Kit (Applied Biological Materials, Richmond, BC, Canada) prior to cDNA

435   synthesis using the 5X All-In-One Master mix (Applied Biological Materials), both

436   according to the manufacturer's instructions. qPCR was performed using a BioRad

437   CFX96 Real-Time System (BioRad Laboratories, Hercules, CA) and data analyzed

438   using BioRad CFX Maestro (v.4.1.2433.1219). CD45 RNA levels were normalized to a

439   cellular control for each sample (28S rRNA). Primer sets are listed in Table 1. All qPCR

440   reactions were run in technical triplicate with corresponding no template and -RT

441   controls, which did not exceed background levels. The delta-delta C_t method was used

20

442   to calculate the relative abundance of CD45 cDNA from HHV6A-infected JJhan cells

443   and 293T cells relative to the uninfected JJhan cell control.

444   Table 1. Primers used in this study.

CD45 qRT4 FWD	AAAAGTGCTCCTCCAAGCCA
CD45 qRT4 REV	TGGGAGGCCTACACTTGACA
28S rRNA 3783F	GTGACGCGCATGAATGGA
28S rRNA 3846R	TGTGGTTTCGCTGGATAGTAGGT

445   *Statistical analysis*

446   Statistical analysis was done using GraphPad 8 (v.8.4.3). One-way ANOVA analysis

447   with Tukey's multiple comparisons test was used to compare the abundance of CD45

448   mRNA 293T cells, uninfected JJhan cells, and HHV6A-infected T cells. **** < 0.0001

449   **Acknowledgements**

References Cited

1. Zerr DM, Meier AS, Selke SS, Frenkel LM, Huang ML, Wald A, Rhoads MP, Nguy L, Bornemann R, Morrow RA, Corey L. 2005. A population-based study of primary human herpesvirus 6 infection. N Engl J Med 352:768-76.

2. Yamanishi K, Shiraki K, Kondo T, Okuno T, Takahashi M, Asano Y, Kurata T. 1988. Identification of human herpesvirus-6 as a causal agent for exanthem subitum The Lancet 331:1065-1067.

3. Omasits U, Ahrens CH, Müller S, Wollscheid B. 2014. Protter: interactive protein feature visualization and integration with experimental proteomic data. Bioinformatics 30:884-6.

4. Emmanual J. Wiertz TRJ, Lei Sun, Matthew Bogyo, Hans J. Geuze, Hidde L. Ploegh. 1996. The Human Cytomegalovirus US11 Gene ProductDislocates MHC Class I Heavy Chainsfrom the Endoplasmic Reticulum to the Cytosol. Cell 84:769-779.

5. Jones TR, Sun L. 1997. Human cytomegalovirus US2 destabilizes major histocompatibility complex class I heavy chains. J Virol 71:2970-2979.

6. Elboim M, Grodzovski I, Djian E, Wolf DG, Mandelboim O. 2013. HSV-2 specifically down regulates HLA-C expression to render HSV-2-infected DCs susceptible to NK cell killing. PLoS Pathog 9:e1003226.

7. Imai T, Koyanagi N, Ogawa R, Shindo K, Suenaga T, Sato A, Arii J, Kato A, Kiyono H, Arase H, Kawaguchi Y. 2013. Us3 kinase encoded by herpes simplex virus 1 mediates downregulation of cell surface major histocompatibility complex class I and evasion of CD8+ T cells. PLoS One 8:e72050.

8. D.J. Schust ABH, H. L. Ploegh. 1996. Herpes simplex virus blocks intracellular transport of HLA-G in placentally derived human cells. Journal of Immunology 157:3375-3380.

9. Früh K, Ahn K, Djaballah H, Sempe P, van Endert P, Tampe R, Peterson P, Yang Y. 1995. A viral inhibitor of peptide transporters for antigen presentation. Nature 375:415-418.

10. A.York CR, D. W. Andrews, S. R. Riddell, F. L. Graham, D. C. Johnson. 1994. A cytosolic herpes simplex virus protein inhibits antigen presentation to CD8+ T lymphocytes Cell 20:525-535.

11. Keating S, Prince S, Jones M, Rowe M. 2002. The lytic cycle of Epstein-Barr virus is associated with decreased expression of cell surface major histocompatibility complex class I and class II molecules. J Virol 76:8179-88.

12. Glosson NL, Hudson A. 2007. Human herpesvirus-6A and -6B encode viral immunoevasins that downregulate class I MHC molecules. Virology 365:125-135.

13. Hudson AW, Howley PM, Ploegh HL. 2001. A human herpesvirus 7 glycoprotein, U21, diverts major histocompatibility complex class I molecules to lysosomes. J Virol 75:12347-58.

14. Dassa L, Seidel E, Oiknine-Djian E, Yamin R, Wolf DG, Le-Trilling VTK, Mandelboim O. 2018. The Human Cytomegalovirus Protein UL148A Downregulates the NK Cell-Activating Ligand MICA To Avoid NK Cell Attack. J Virol 92.

15. Seidel E, Le VTK, Bar-On Y, Tsukerman P, Enk J, Yamin R, Stein N, Schmiedel D, Oiknine Djian E, Weisblum Y, Tirosh B, Stastny P, Wolf DG, Hengel H, Mandelboim O. 2015. Dynamic Co-evolution of Host and Pathogen: HCMV Downregulates the Prevalent Allele MICA∗008 to Escape Elimination by NK Cells. Cell Rep 10:968-982.

22

509
510   16.   Fielding CA, Aicheler R, Stanton RJ, Wang EC, Han S, Seirafian S, Davies J, McSharry BP, Weekes MP,
511   Antrobus PR, Prod'homme V, Blanchet FP, Sugrue D, Cuff S, Roberts D, Davison AJ, Lehner PJ, Wilkinson
512   GW, Tomasec P. 2014. Two novel human cytomegalovirus NK cell evasion functions target MICA for
513   lysosomal degradation. PLoS Pathog 10:e1004058.
514
515   17.   Stern-Ginossar N, Elefant N, Zimmermann A, Wolf DG, Saleh N, Biton M, Horwitz E, Prokocimer Z, Prichard
516   M, Hahn G, Goldman-Wohl D, Greenfield C, Yagel S, Hengel H, Altuvia Y, Margalit H, Mandelboim O. 2007.
517   Host immune system gene targeting by a viral miRNA. Science 317:376-81.
518
519   18.   Rölle A, Mousavi-Jazi M, Eriksson M, Odeberg J, Söderberg-Nauclér C, Cosman D, Kärre K, Cerboni C. 2003.
520   Effects of human cytomegalovirus infection on ligands for the activating NKG2D receptor of NK cells: up-
521   regulation of UL16-binding protein (ULBP)1 and ULBP2 is counteracted by the viral UL16 protein. The
522   Journal of Immunology 171:902-908.
523
524   19.   Schneider CL, Hudson A. 2011. The human herpesvirus-7 (HHV-7) U21 immunoevasin subverts NK-
525   mediated cytoxicity through modulation of MICA and MICB. PLoS Pathog 7:e1002362.
526
527   20.   Anders S, Huber W. 2010. Differential expression analysis for sequence count data. Genome Biol 11:R106.
528
529   21.   Bonifacino JS, Dell'Angelica EC. 2001. Immunoprecipitation. Current protocols in cell biology / editorial
530   board, Juan S Bonifacino [et al] Chapter 7:Unit 7.2.
531
532   22.   Peretti S, Shaw A, Blanchard J, Bohm R, Morrow G, Lifson JD, Gettie A, Pope M. 2005. Immunomodulatory
533   effects of HSV-2 infection on immature macaque dendritic cells modify innate and adaptive responses.
534   Blood 106:1305-13.
535
536   23.   Morrow G, Slobedman B, Cunningham AL, Abendroth A. 2003. Varicella-zoster virus productively infects
537   mature dendritic cells and alters their immune function. J Virol 77:4950-9.
538
539   24.   Mikloska Z, Bosnjak L, Cunningham AL. 2001. Immature monocyte-derived dendritic cells are productively
540   infected with herpes simplex virus type 1. J Virol 75:5958-64.
541
542   25.   Andrews DM, Andoniou CE, Granucci F, Ricciardi-Castagnoli P, Degli-Esposti MA. 2001. Infection of
543   dendritic cells by murine cytomegalovirus induces functional paralysis. Nat Immunol 2:1077-84.
544
545   26.   Salio M, Cella M, Suter M, Lanzavecchia A. 1999. Inhibition of dendritic cell maturation by herpes simplex
546   virus. Eur J Immunol 29:3245-53.
547
548   27.   Jones D, Como CN, Jing L, Blackmon A, Neff CP, Krueger O, Bubak AN, Palmer BE, Koelle DM, Nagel MA.
549   2019. Varicella zoster virus productively infects human peripheral blood mononuclear cells to modulate
550   expression of immunoinhibitory proteins and blocking PD-L1 enhances virus-specific CD8+ T cell effector
551   function. PLoS Pathog 15:e1007650.
552
553   28.   Gilardini Montani MS, Santarelli R, Falcinelli L, Gonnella R, Granato M, Di Renzo L, Cuomo L, Vitillo M,
554   Faggioni A, Cirone M. 2018. EBV up-regulates PD-L1 on the surface of primary monocytes by increasing
555   ROS and activating TLR signaling and STAT3. J Leukoc Biol 104:821-832.
556
557   29.   Host KM, Jacobs SR, West JA, Zhang Z, Costantini LM, Stopford CM, Dittmer DP, Damania B. 2017. Kaposi's
558   Sarcoma-Associated Herpesvirus Increases PD-L1 and Proinflammatory Cytokine Expression in Human
559   Monocytes. mBio 8.
560

30. McSharry BP, Forbes SK, Cao JZ, Avdic S, Machala EA, Gottlieb DJ, Abendroth A, Slobedman B. 2014. Human cytomegalovirus upregulates expression of the lectin galectin 9 via induction of beta interferon. J Virol 88:10990-4.

31. Reddy PB, Sehrawat S, Suryawanshi A, Rajasagi NK, Mulik S, Hirashima M, Rouse BT. 2011. Influence of galectin-9/Tim-3 interaction on herpes simplex virus-1 latency. J Immunol 187:5745-55.

32. Benedict CA, Loewendorf A, Garcia Z, Blazar BR, Janssen EM. 2008. Dendritic cell programming by cytomegalovirus stunts naive T cell responses via the PD-L1/PD-1 pathway. J Immunol 180:4836-47.

33. Weekes MP, Tomasec P, Huttlin EL, Fielding CA, Nusinow D, Stanton RJ, Wang ECY, Aicheler R, Murrell I, Wilkinson GWG, Lehner PJ, Gygi SP. 2014. Quantitative temporal viromics: an approach to investigate host-pathogen interaction. Cell 157:1460-1472.

34. Bartee E, McCormack A, Früh K. 2006. Quantitative membrane proteomics reveals new cellular targets of viral immune modulators. PLoS Pathog 2:e107.

35. Hertel L, Lacaille VG, Strobl H, Mellins ED, Mocarski ES. 2003. Susceptibility of immature and mature Langerhans cell-type dendritic cells to infection and immunomodulation by human cytomegalovirus. J Virol 77:7563-74.

36. Coscoy L, Ganem D. 2001. A viral protein that selectively downregulates ICAM-1 and B7-2 and modulates T cell costimulation. J Clin Invest 107:1599-606.

37. Mansouri M, Douglas J, Rose PP, Gouveia K, Thomas G, Means RE, Moses AV, Früh K. 2006. Kaposi sarcoma herpesvirus K5 removes CD31/PECAM from endothelial cells. Blood 108:1932-40.

38. MacLean B, Tomazela DM, Shulman N, Chambers M, Finney GL, Frewen B, Kern R, Tabb DL, Liebler DC, MacCoss MJ. 2010. Skyline: an open source document editor for creating and analyzing targeted proteomics experiments. Bioinformatics 26:966-8.

39. Rheinlander A, Schraven B, Bommhardt U. 2018. CD45 in human physiology and clinical medicine. Immunol Lett 196:22-32.

40. Holmes N. 2006. CD45: all is not yet crystal clear. Immunology 117:145-55.

41. Hermiston ML, Xu Z, Weiss A. 2003. CD45: a critical regulator of signaling thresholds in immune cells. Annu Rev Immunol 21:107-37.

42. Sasaki T, Sasaki-Irie J, Penninger JM. 2001. New insights into the transmembrane protein tyrosine phosphatase CD45. Int J Biochem Cell Biol 33:1041-6.

43. Koretzky GA, Picus J, Schultz T, Weiss A. 1991. Tyrosine phosphatase CD45 is required for T-cell antigen receptor and CD2-mediated activation of a protein tyrosine kinase and interleukin 2 production. Proc Natl Acad Sci U S A 88:2037-41.

44. Koretzky GA, Picus J, Thomas ML, Weiss A. 1990. Tyrosine phosphatase CD45 is essential for coupling T-cell antigen receptor to the phosphatidyl inositol pathway. Nature 346:66-8.

45. Pingel JT, Thomas ML. 1989. Evidence that the leukocyte-common antigen is required for antigen-induced T lymphocyte proliferation. Cell 58:1055-65.

612   46.   Fujinaka CM, Waas M, Gundry RL. 2018. Mass Spectrometry-Based Identification of Extracellular Domains
613   of Cell Surface N-Glycoproteins: Defining the Accessible Surfaceome for Immunophenotyping Stem Cells
614   and Their Derivatives. Methods Mol Biol 1722:57-78.
615

616   47.   Mallanna SK, Waas M, Duncan SA, Gundry RL. 2017. N-glycoprotein surfaceome of human induced
617   pluripotent stem cell derived hepatic endoderm. Proteomics 17.
618

619   48.   Mallanna SK, Cayo MA, Twaroski K, Gundry RL, Duncan SA. 2016. Mapping the Cell-Surface N-
620   Glycoproteome of Human Hepatocytes Reveals Markers for Selecting a Homogeneous Population of iPSC-
621   Derived Hepatocytes. Stem Cell Reports 7:543-556.
622

623   49.   Boheler KR, Bhattacharya S, Kropp EM, Chuppa S, Riordon DR, Bausch-Fluck D, Burridge PW, Wu JC,
624   Wersto RP, Chan GC, Rao S, Wollscheid B, Gundry RL. 2014. A human pluripotent stem cell surface N-
625   glycoproteome resource reveals markers, extracellular epitopes, and drug targets. Stem Cell Reports
626   3:185-203.
627

628   50.   Wollscheid B, Bausch-Fluck D, Henderson C, O'Brien R, Bibel M, Schiess R, Aebersold R, Watts JD. 2009.
629   Mass-spectrometric identification and relative quantification of N-linked cell surface glycoproteins. Nat
630   Biotechnol 27:378-86.
631

632   51.   Pawelec G, Borowitz A, Krammer PH, Wernet P. 1982. Constitutive interleukin 2 production by the JURKAT
633   human leukemic T cell line. Eur J Immunol 12:387-392.
634

635   52.   Dölken L, Krmpotić A, Kothe S, Tuddenham L, Tanguy M, Marcinowski L, Ruzsics Z, Elefant N, Altuvia Y,
636   Margalit H, Koszinowski UH, Jonjić S, Pfeffer S. 2010. Cytomegalovirus microRNAs facilitate persistent
637   virus infection in salivary glands. PLoS Pathog 6:e1001150.
638

639   53.   Hall LR, Streuli M, Schlossman SF, Saito H. 1988. Complete exon-intron organization of the human
640   leukocyte common antigen (CD45) gene. J Immunol 141:2781-7.
641

642   54.   Streuli M, Hall LR, Saga Y, Schlossman SF, Saito H. 1987. Differential usage of three exons generates at
643   least five different mRNAs encoding human leukocyte common antigens. J Exp Med 166:1548-66.
644

645   55.   Ralph SJ, Thomas ML, Morton CC, Trowbridge IS. 1987. Structural variants of human T200 glycoprotein
646   (leukocyte-common antigen). Embo j 6:1251-7.
647

648   56.   Rothstein DM, Saito H, Streuli M, Schlossman SF, Morimoto C. 1992. The alternative splicing of the CD45
649   tyrosine phosphatase is controlled by negative regulatory trans-acting splicing factors. J Biol Chem
650   267:7139-47.
651

652   57.   Sullivan BM, Coscoy L. 2008. Downregulation of the T-cell receptor complex and impairment of T-cell
653   activation by human herpesvirus 6 u24 protein. J Virol 82:602-8.
654

655   58.   Nicholas J. 1996. Determination and analysis of the complete nucleotide sequence of human herpesvirus-
656   7. J Virol 70:5975-5989.
657

658   59.   Isegawa Y, Mukai T, Nakano K, Kagawa M, Chen J, Mori Y, Sunagawa T, Kawanishi K, Sashihara J, Hata A,
659   Zou P, Kosuge H, Yamanishi K. 1999. Comparison of the complete DNA sequences of human herpesvirus 6
660   variants A and B. J Virol 73:8053-63.
661

662   60.   Thiel N, Keyser KA, Lemmermann NA, Oduro JD, Wagner K, Elsner C, Halenius A, Lenac Rovis T, Brinkmann
663   MM, Jonjic S, Cicin-Sain L, Messerle M. 2016. The Mouse Cytomegalovirus Gene m42 Targets Surface

25

664   Expression of the Protein Tyrosine Phosphatase CD45 in Infected Macrophages. PLoS Pathog
665   12:e1006057.
666
667   61.   Mustelin T, Coggeshall KM, Altman A. 1989. Rapid activation of the T-cell tyrosine protein kinase pp56lck
668   by the CD45 phosphotyrosine phosphatase. Proc Natl Acad Sci U S A 86:6302-6.
669
670   62.   Mustelin T, Altman A. 1990. Dephosphorylation and activation of the T cell tyrosine kinase pp56lck by the
671   leukocyte common antigen (CD45). Oncogene 5:809-13.
672
673   63.   Mustelin T, Pessa-Morikawa T, Autero M, Gassmann M, Andersson LC, Gahmberg CG, Burn P. 1992.
674   Regulation of the p59fyn protein tyrosine kinase by the CD45 phosphotyrosine phosphatase. Eur J
675   Immunol 22:1173-8.
676
677   64.   Gabaev I, Steinbruck L, Pokoyski C, Pich A, Stanton RJ, Schwinzer R, Schulz TF, Jacobs R, Messerle M, Kay-
678   Fedorov PC. 2011. The human cytomegalovirus UL11 protein interacts with the receptor tyrosine
679   phosphatase CD45, resulting in functional paralysis of T cells. PLoS Pathog 7:e1002432.
680
681   65.   Zischke J, Mamareli P, Pokoyski C, Gabaev I, Buyny S, Jacobs R, Falk CS, Lochner M, Sparwasser T, Schulz
682   TF, Kay-Fedorov PC. 2017. The human cytomegalovirus glycoprotein pUL11 acts via CD45 to induce T cell
683   IL-10 secretion. PLoS Pathog 13:e1006454.
684
685   66.   Arena A, Liberto MC, Iannello D, Capozza AB, Focà A. 1999. Altered cytokine production after human
686   herpes virus type 6 infection. New Microbiol 22:293-300.
687
688   67.   Li C, Goodrich JM, Yang X. 1997. Interferon-gamma (IFN-gamma) regulates production of IL-10 and IL-12 in
689   human herpesvirus-6 (HHV-6)-infected monocyte/macrophage lineage. Clin Exp Immunol 109:421-5.
690
691   68.   Windheim M, Southcombe JH, Kremmer E, Chaplin L, Urlaub D, Falk CS, Claus M, Mihm J, Braithwaite M,
692   Dennehy K, Renz H, Sester M, Watzl C, Burgert HG. 2013. A unique secreted adenovirus E3 protein binds
693   to the leukocyte common antigen CD45 and modulates leukocyte functions. Proc Natl Acad Sci U S A
694   110:E4884-93.
695
696   69.   Sanyal A, Wallaschek N, Glass M, Flamand L, Wight DJ, Kaufer BB. 2018. The ND10 Complex Represses
697   Lytic Human Herpesvirus 6A Replication and Promotes Silencing of the Viral Genome. Viruses 10.
698
699   70.   Courtney AH, Amacher JF, Kadlecek TA, Mollenauer MN, Au-Yeung BB, Kuriyan J, Weiss A. 2017. A
700   Phosphosite within the SH2 Domain of Lck Regulates Its Activation by CD45. Mol Cell 67:498-511.e6.
701
702   71.   Tang H, Kawabata A, Yoshida M, Oyaizu H, Maeki T, Yamanishi K, Mori Y. 2010. Human herpesvirus 6
703   encoded glycoprotein Q1 gene is essential for virus growth. Virology 407:360-367.
704
705   72.   May NA, Wang Q, Balbo A, Konrad SL, Buchli R, Hildebrand WH, Schuck P, Hudson AW. 2014. Human
706   herpesvirus 7 U21 tetramerizes to associate with class I major histocompatibility complex molecules. J
707   Virol 88:3298-308.
708
709   73.   Waas M, Pereckas M, Jones Lipinski RA, Ashwood C, Gundry RL. 2019. SP2: Rapid and Automatable
710   Contaminant Removal from Peptide Samples for Proteomic Analyses. J Proteome Res 18:1644-1656.
711
712   74.   Mihara K, Nakayama T, Saitoh H. 2015. A Convenient Technique to Fix Suspension Cells on a Coverslip for
713   Microscopy. Curr Protoc Cell Biol 68:4 30 1-4 30 10.
714